Available online at www.sciencedirect.com
SCIENCE DIRECT®
ELSEVIER
Journal of Magnetism and Magnetic Materials 290–291 (2005) 779–782
Journal of magnetism and magnetic materials
www.elsevier.com/locate/jmmm

Magnetic structure of cross-shaped permalloy arrays embedded in silicon wafers

Kenji Machida[a,b,*], Tomoyuki Tezuka[b], Takahiro Yamamoto[b], Takayuki Ishibashi[b], Yoshitaka Morishita[b], Akinori Koukitu[b], Katsuaki Sato[b]

[a] *Materials Science, Science & Technical Research Laboratories, NHK, Setagaya-ku, Tokyo 157-8510, Japan*
[b] *Faculty of Technology, Tokyo University of Agriculture and Technology, Koganei, Tokyo 184-8588, Japan*

Available online 14 December 2004

Abstract

This paper describes the observed magnetic structure and the micromagnetic simulation of cross-shaped, permalloy ($Ni_{80}Fe_{20}$) arrays embedded in silicon wafers. The nano-scale-width, cross-shaped patterns were fabricated using the damascene technique, electron beam lithography, and chemical mechanical polishing. The magnetic poles were observed as two pairs of bright and dark spots at the ends of the crossed-bars using a magnetic force microscope. The force gradient distributions were simulated based on micromagnetic calculations and tip's stray field calculations using the integral equation method. This process of calculation successfully explains the appearance of the poles and complicated spin structure at the crossing region.

PACS: 75.60.Ch; 75.75.+a

Keywords: Magnetic structure; Micromagnetic simulation; Damascene technique; Magnetic force microscope

It is critical to understand the spin structures and magnetic switching behavior of nano-scale patterned magnetic elements for application in high-density data storage devices, nonvolatile magnetic memories, and magnetic logic gates. The spin structures of square, rectangular, and circular dots have been extensively studied [1]. We have investigated regularly aligned magnetic patterns of square ($1 \times 1\,\mu m^2$), rectangular ($300 \times 100\,nm^2$), and circular (100 nm in diameter) arrays with a thickness of 150 nm and a pattern separation of 300 nm embedded in silicon wafers [2]. These patterns were successfully fabricated using the damascene technique, electron beam (EB) lithography, and chemical mechanical polishing (CMP). However, the spin structures for more complicated geometries with a branch have not yet been adequately investigated. We focused on cross-shaped arrays of permalloy ($Ni_{80}Fe_{20}$) in order to clarify their spin structures.

Fig. 1 shows the mask patterns of the cross-shaped arrays. Two kinds of structures termed CROSS1 (200 nm in width, 3 μm in length with a separation of 3 μm) and CROSS2 (100 nm in width, 1.5 μm in length with a separation of 1.5 μm) were fabricated. EB resist films (ZEP520) spin-coated on a silicon wafer were exposed. The wafer with the patterned resist films was dry-etched by RIE using CF_4 gas, and pit arrays of about 150 nm in depth were formed on the wafer. Permalloy films were deposited on to the pit arrays using

*Corresponding author. Materials Science, Science & Technical Research Laboratories, NHK 1-10-11 Kinuta, Setagaya-ku, Tokyo 157-8510, Japan. Tel.: +81 3 5494 3254; fax: +81 3 5494 3261.
E-mail address: machida.k-ge@nhk.or.jp (K. Machida).

0304-8853/$ - see front matter © 2004 Elsevier B.V. All rights reserved.
doi:10.1016/j.jmmm.2004.11.404

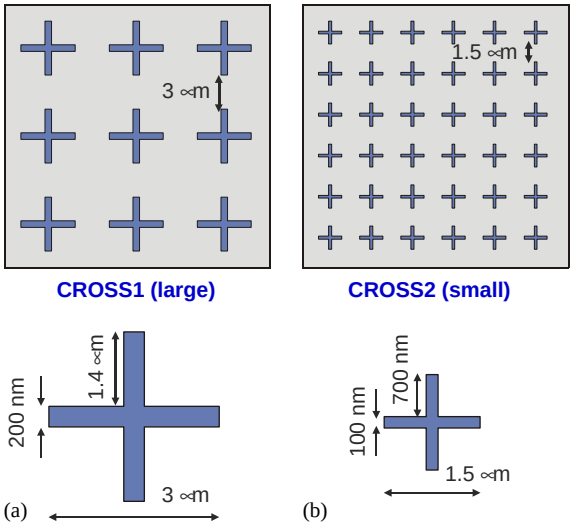

Fig. 1. Mask patterns of cross-shaped arrays for (a) CROSS1 (200 nm in width, 3 μm in length with separation of 3 μm) and (b) CROSS2 (100 nm in width, 1.5 μm in length with separation of 1.5 μm).

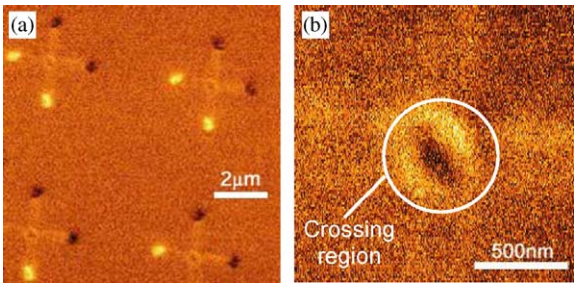

Fig. 2. MFM images for CROSS1 measured in high vacuum with low-moment tip (a) in $10 \times 10\,\mu m^2$ scan area and (b) in $1.5 \times 1.5\,\mu m^2$ scan area.

an electron beam evaporator, and the films outside the pit were polished out by CMP.

The remanent state of these nano-scale arrays was observed using an SII Nanotechnology model SPI-4000/SPA300HV magnetic force microscope (MFM) system with a low-moment probe (having a 24-nm-thick Co–Cr–Pt coated tip) using a specially designed Q-control in high vacuum, after applying a magnetic field of 20 kOe in the direction toward the tip from the sample.

Figs. 2(a) and (b) show MFM images for CROSS1 measured in $10 \times 10\,\mu m^2$ scan area and in $1.5 \times 1.5\,\mu m^2$ scan area, respectively. The magnetic poles were observed as two pairs of bright and dark spots at the ends of the crossed-bars in Fig. 2(a). Fig. 2(b) shows a magnified image around the crossing region. A complicated MFM image was observed, that is, bright and dark contrasts appeared on each side of a slanted boundary in the crossing region.

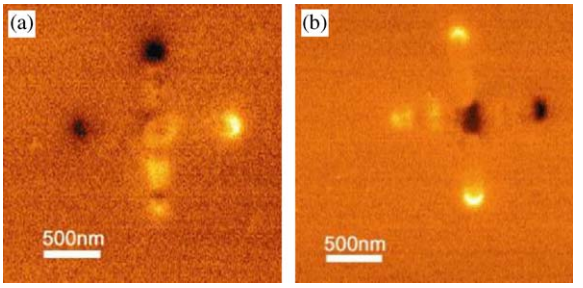

Fig. 3. (a) MFM image of one dot and (b) another dot in the CROSS2 patterns, measured in high vacuum with low-moment tip.

Figs. 3(a) and (b) show the MFM image of one dot and that of another dot in the CROSS2 patterns, respectively. The bright and dark spots at the bar-ends of each dot appeared in a different configuration from that of CROSS1, which may be attributed to the smaller cross-patterns irregular in shape such as variations in width or depth of the bars, limited by the resolution of the EB lithography.

Micromagnetic calculations using the Landau–Lifshitz–Gilbert equation were done to explain the observed MFM images of the cross-shaped nano-scale patterns. The micromagnetic simulator [3] was modified to correspond to a complicated three-dimensional (3D) pattern, which was created using a generic 3D-CAD system. The equation was numerically solved using the fourth order Runge–Kutta method for high accuracy.

Fig. 4(a) shows the magnetization configuration of a cross-shaped pattern 100 nm in width, 1.5 μm in length, and 100 nm in depth, corresponding to the pattern of CROSS2. The elementary volume is a 20 nm cubic. The arrow and gradation shown as a background image represent the magnetization vectors and $-\mathrm{div}\,\boldsymbol{M}$, respectively. The magnetization of each of the crossed-bars was aligned in the direction of the long side, due to shape anisotropy. The magnetization direction at the crossing region is thereby aligned in the direction from the top right to the bottom left. Fig. 4(b) shows the diagonal view rotated around the y-axis. The vortex structures were formed in the z-direction at each end of the crossed bars.

To demonstrate the MFM images, it is necessary to consider the interaction between the magnetization of the tip and the stray field of the sample. The MFM output signals are proportional to the force gradient between the tip and the sample. The force gradient is given by [4]

$$\frac{\delta F_z}{\delta z_{\mathrm{tip}}} = \int_{\mathrm{sample}} \frac{\partial^2 \boldsymbol{H}_{\mathrm{tip}}}{\partial z^2} \cdot \boldsymbol{M}_{\mathrm{sample}}\, \mathrm{d}^3 r + \int_{\mathrm{sample}} \frac{\partial \boldsymbol{H}_{\mathrm{tip}}}{\partial z} \cdot \frac{\delta \boldsymbol{M}_{\mathrm{sample}}}{\delta z_{\mathrm{tip}}}\, \mathrm{d}^3 r, \quad (1)$$

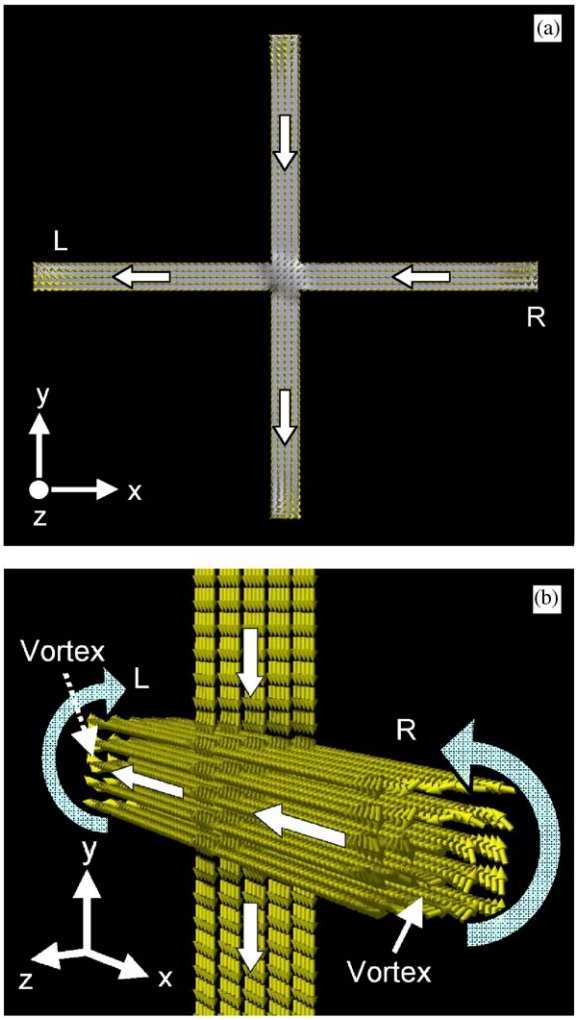

Fig. 4. (a) Calculated magnetization configuration for cross-shaped permalloy pattern, (b) rotated around y-axis.

where $\boldsymbol{H}_{\text{tip}}$ is the stray field from the tip at the sample volume element, $\boldsymbol{M}_{\text{sample}}$ is the magnetization of a sample volume element at equilibrium, and z_{tip} is the tip–sample distance. The values of $\boldsymbol{H}_{\text{tip}}$ and $\boldsymbol{M}_{\text{sample}}$ are considered to change corresponding to the tip–sample interaction. The magnitude of the coercive force (H_c) for a 24-nm-thick Co–Cr–Pt coated tip is about 650 Oe. Therefore, the influence of a sample's stray field on the magnetization of the hard magnetic tip is considered to be approximately constant. On the other hand, the influence of a tip's stray field on the magnetization of the soft magnetic sample, that is, $\delta\boldsymbol{M}_{\text{sample}}/\delta z_{\text{tip}}$ included in the second term of Eq. (1), is considerably large. However, in this work, this term was excluded to save calculation time.

Fig. 5 shows the schematic structure of the MFM probe model for calculating $\boldsymbol{H}_{\text{tip}}$ at the sample's volume

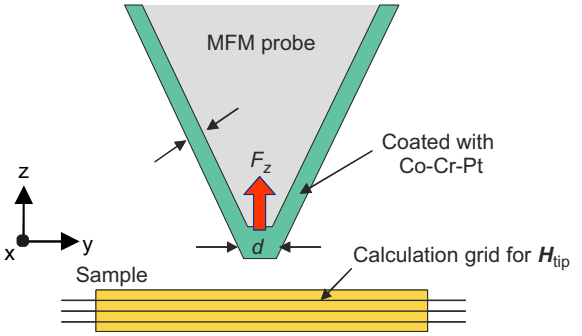

Fig. 5. Schematic structure of MFM probe model for calculating $\boldsymbol{H}_{\text{tip}}$ at sample's volume element.

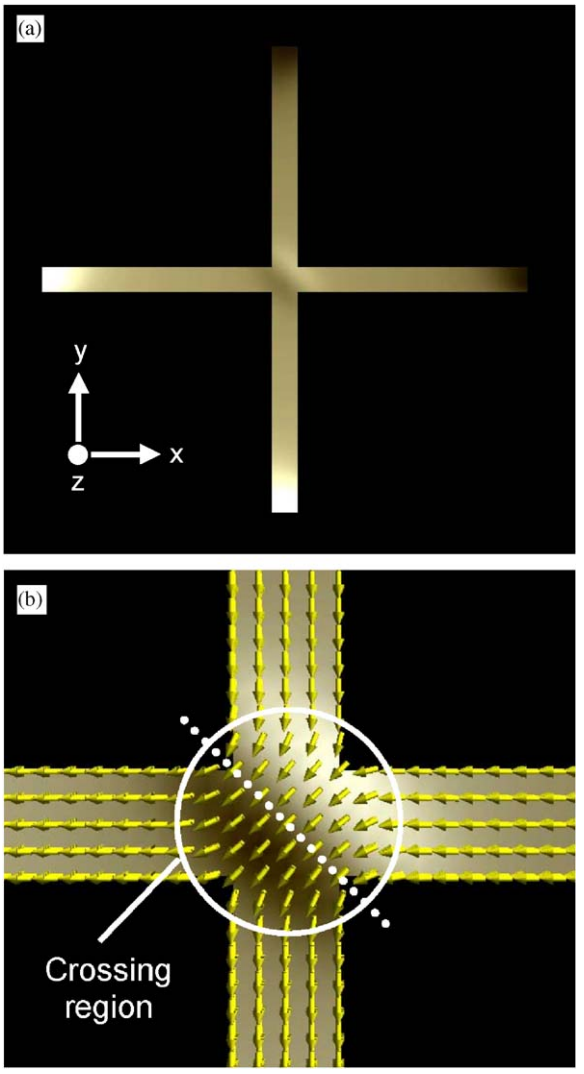

Fig. 6. (a) Force gradient distribution of cross-shaped permalloy pattern and (b) with magnetization distribution at crossing region.

element. The MFM probe's tip (tip diameter $d = 30\,\mathrm{nm}$) is coated with Co–Cr–Pt (thickness $t = 24\,\mathrm{nm}$ and $H_c = 650\,\mathrm{Oe}$). The $\boldsymbol{H}_{\mathrm{tip}}$ distributions were calculated using an integral equation method.

Fig. 6 shows the force gradient distributions of a cross-shaped pattern. Two pairs of bright and dark spots were obtained at the ends of the crossed-bars, as shown in Fig. 6(a). Furthermore, as shown in Fig. 6(b), bright and dark contrasts appeared on each side of a slanted boundary (the dotted line) in the crossing region, consistent with the experimental MFM image shown in Fig. 2(b), even though the size of the simulated pattern is different from that of the CROSS1 pattern shown in Fig. 2(b).

In conclusion, cross-shaped permalloy arrays embedded in silicon wafers were fabricated using the damascene technique, and their spin structures were investigated using MFM measurements. The force gradient distributions for a cross-shaped pattern were simulated based on micromagnetic calculations and tip's stray field calculations using the integral equation method. This process of calculation successfully explains the important features of MFM images; i.e., appearance of magnetic poles at the bar ends, and the complicated spin structure at the crossing region.

The authors are very grateful to Dr. T. Yamaoka of SII Nanotechnology Inc. for his kind permission to use the MFM machine with a low-moment tip. This research has been conducted under the 21st-century COE program of TUAT on "Future Nano Materials".

References

[1] A. Hubert, R. Schäfer, Magnetic Domains—The Analysis of Magnetic Microstructures, Springer, New York, 1998.
[2] T. Matsumoto, T. Tezuka, T. Ishibashi, Y. Morishita, A. Koukitu, K. Sato, Trans. Magn. Soc. Jpn. 3 (2003) 103.
[3] K. Machida, N. Hayashi, Y. Yoneda, J. Numazawa, M. Kohro, T. Tanabe, J. Magn. Magn. Mater. 226–230 (2001) 2054.
[4] J.M. García, A. Thiaville, J. Miltat, K.J. Kirk, J.N. Chapman, F. Alouges, Appl. Phys. Lett. 79 (2001) 656.